Novel tools for protein phosphorylation analysis based on proton release detection: potential tools for drug discovery

Nikhil Bhalla[1], Mirella Di Lorenzo[2], Giordano Pula[3], Pedro Estrela[1,*]

[1]Department of Electronic & Electrical Engineering, University of Bath, Bath BA2 7AY, United Kingdom; Email: N.Bhalla@bath.ac.uk, P.Estrela@bath.ac.uk

[2]Department of Chemical Engineering, University of Bath, Bath BA2 7AY, United Kingdom; Email: M.Di.Lorenzo@bath.ac.uk

[3]Department of Pharmacy & Pharmacology, University of Bath, Bath BA2 7AY, United Kingdom; Email: G.Pula@bath.ac.uk

*Corresponding author: Department of Electronic & Electrical Engineering, University of Bath, Claverton Down, Bath, BA2 7AY, United Kingdom
E-mail: P.Estrela@bath.ac.uk
Phone: +44-1225-386324

Abstract

Phosphorylation is the most important post-translational modification of proteins in eukaryotic cells and it is catalysed by enzymes called kinases. The balance between protein phosphorylation and dephosphorylation is critical for the regulation of physiological processes and its unbalance is the cause of several diseases. Conventional assays used to analyse the kinase activity are limited as they rely heavily on phospho-specific antibodies and radioactive tags. This makes their use impractical for high throughput drug discovery platforms. We have developed two versatile methods to detect the release of protons (H^+) associated with the protein phosphorylation catalysed by kinases. The first approach is based on the pH-sensitive response of oxide-semiconductor interfaces and the second method detects the pH changes in phosphorylation reaction using a commercial micro pH electrode. The proposed methods successfully detected phosphorylation of myelin basic protein by PKC-α kinase. These techniques can be readily adopted for multiplexed arrays and high throughput analysis of kinase activity, which will represent an important innovation in biomedical research and drug discovery.

Introduction

Serine, threonine and tyrosine amino acids can be phosphorylated by protein kinases, which regulate protein conformation, trafficking, degradation and activity (Cohen, 2002; Groban *et al.*, 2006). Protein phosphorylation plays a critical role in the regulation of cell growth, differentiation and apoptosis (Manning *et al.*, 2002), while its dysregulation is the cause of many diseases (Cohen, 2001). Autoimmune disorders (Arsenault *et al.*, 2011; Kobashigawa *et al.*, 2011), chronic inflammatory diseases (Cohen, 2001; Martinez *et al.*, 2002), different cancers (Chen *et al.*, 2009), diabetes (Cohen, 2001) and Alzheimer's disease (Buxbaum, 1993; Wang *et al.*, 2013) are associated with abnormal protein phosphorylation. In this respect, kinase inhibitors are intensively investigated in drug discovery (Cohen and Alessi, 2013). Current methods for understanding kinase activity are based on mass spectroscopy (Zhang *et al.*, 2005), electrochemical impedance spectroscopy (Martić *et al.*, 2012a, 2012b), isotope labelling technique (Stasyk and Huber, 2012), or immunoassays (Nadler et al., 2008). The above techniques are time consuming, laborious, cost inefficient or require the usage of toxic chemical reagents (e.g. radioactive tags/labels). Alternative approaches have been proposed such as cyclic voltammetry (Wang *et al.*, 2010), contact angle measurements (Wieckowska *et al.*, 2008), surface plasmon resonance (Yoshida *et al.*, 2000), fluorescence polarisation (Inoue *et al.*, 2002) nanoparticle-based approaches (Kerman and Kraatz, 2009), and electrogenerated chemiluminescence (Chen *et al.*, 2013). These label-free electrochemical or optical techniques avoid some of these limitations and could precisely determine the kinase activity (Wang *et al.*, 2011; Miao *et al.*, 2012). However, most of these methods have so far found limited application because in the vast majority they are unsuitable for high-throughput screening (HTS), and often require highly specialised and expensive equipment (Mark *et al.*, 2010).

Field-effect transistor (FET) devices as electronic transducers for label-free detection of bimolecular interactions are very promising towards the development of low-cost high-throughput label-free electronic devices. The potential of very large scale integration (VLSI) technology to form an array of ion-sensitive FETs (ISFETs) to monitor biocatalytic transformation was explored by Ion Torrent for DNA sequencing on a chip, which allows sequencing at a whole genome level (Rothberg *et al.*, 2011).

This revolutionary technique is based on the creation of a nanoarray of ISFETs, which allows the detection of release of protons from phosphodiester bond formation on thousands of copy DNA molecules at once, leading to the parallel sequencing of several thousands of DNA molecules. A similar approach could be applied to protein phosphorylation studies aiming at either identifying the subset of proteins phosphorylated by a single kinase (one kinase/several potential target proteins) (Lindsay, 2012) or investigating a large number of potential inhibitors/modulators on the activity of a single kinase (one kinase/one target protein). The latter would make possible to identify novel protein kinase inhibitors and its application in the development of miniaturised drug discovery platforms can be envisaged. For example, FETs were used to measure the charge of phosphorylated proteins from kinase activity (Freeman *et al.*, 2007), where the degree of charging of the gate surface on FET structures due to kinase activity was studied. An alternative and arguably simpler approach would be to directly monitor the pH changes that occur upon phosphorylation; such pH monitoring could be achieved by e.g. the use of field-effect devices or micro pH meters.

We report here on two methods used to detect protein phosphorylation of myelin basic protein by the Protein Kinase C alpha (PKC-α) kinase. In one method (Fig. 1), we employ the use of electrolyte–insulator–semiconductor (EIS) capacitor structures to detect the release of protons (H^+) associated with the protein phosphorylation. This is detected in terms of changes in gate capacitance at the oxide-semiconductor interface, which in turn modulates the gate bias voltage of the EIS capacitor. In the second method we use a commercial micro pH electrode to measure changes in pH associated with protein phosphorylation. We also performed western blot to confirm the kinase activity and identity optimum conditions for phosphorylation on the semiconductor structures.

Materials and Methods

Reagents

All chemicals were of analytical grade and were used as received, unless otherwise specified. All aqueous solutions were made with double de-ionised water, 18.2 MΩ cm, with a Pyrogard filter

(Millipore, USA). Tris base, $MgCl_2$, NaCl, acetone, NH_4OH, HCl, H_2O_2, 3-glycidoxypropyltrimethoxysilane (GOPTS), PKC-α kinase inhibitor GF 109203X, adenosine tri-phosphate (ATP) and 3,3´,5,5´-tetramentylbenzidine (TMB) were purchased from Sigma-Aldrich. Dephosphorylated myelin basic protein (MBP), purified from bovine brain using fast protein liquid chromatography (FPLC), was purchased from Millipore. PKC-α human recombinant kinase produced in Sf9, was procured from ProSec-Tray TechnoGene Ltd. PKC lipid activator cocktail was obtained from Millipore. Polyclonal phospho-(Ser) PKC substrate antibody was purchased from Cell Signaling Technology. Horseradish peroxidase (HRP)-linked anti-rabbit IgG (NA934V) and anti-goat IgG (sc-2020) were bought from GE Healthcare and Santa Cruz Biotechnology, respectively. MBP Antibody (C-16) goat polyclonal IgG 200 µg/ml (sc-139140) was purchased from Santa Cruz Biotechnology.

Si_3N_4 sample preparation

Hundred nanometre of Si_3N_4 was deposited by plasma-enhanced chemical vapour deposition (PECVD) onto 4-inch n-type Si wafers with 50 nm of SiO_2. The Si-SiO_2-Si_3N_4 wafer was cleaned using a standard RCA wafer cleaning protocol. Briefly, the wafer was firstly rinsed with ultra-pure deionised (DI) water and then immersed in 1:1:5 solution of NH_4OH: H_2O_2: DI at 80°C for 10 minutes to remove organic contaminants. Afterwards, to remove inorganic contaminants, the wafer was socked in 1:1:6 solution of HCl: H_2O_2: DI at 80°C for 10 minutes; finally the wafer was rinsed with DI. After cleaning the wafer, 100 nm aluminium was physically deposited on the back of the Si wafer to serve as an ohmic back-contact using an Edwards e-beam evaporator. After aluminium deposition, the Si_3N_4 surface was cleaned using acetone vapour at 110°C. The wafer was sandwiched between a teflon well with an o-ring and a conductive plate (copper), so that the aluminium coated side of the wafer sits on the lower conductive plate. This formed a planar Si_3N_4 well with 19.64 mm^2 interrogation area for the reaction defined by the size of the o-ring (5 mm diameter).

Bio-functionalisation of Si_3N_4

The dried and acetone vapour cleaned Si_3N_4 samples were silanised by incubation in 98% 3-glycidoxypropyltrimethoxysilane (GOPTS) in aqueous solution for 1 hour. Five microliters of 156 µM myelin basic protein (MBP) was dispensed on the silanised Si_3N_4 surface inside the teflon

well for 40 minutes, enabling the amino groups of MBP to attach to the epoxide group of GOPTS. The unreacted GOPTS sites were blocked by incubating the sample in 20% ethanol for 30 minutes. The epoxide converts to ether when reacted with alcohol (Piehler *et al.*, 2000).

Protein phosphorylation on Si_3N_4

PKC-α is a key protein kinase in several physio-pathological events and was selected for this study. Myelin basic protein is a known substrate of PKC-α. Phosphorylation of MBP was carried out in both "complete reaction buffer" (1 mM Tris base, pH 7.4, 30 mM NaCl and 2 mM $MgCl_2$) and "low ionic strength buffer" (0.2 mM Tris base, pH 7.4, 6 mM NaCl and 0.4 mM $MgCl_2$). The whole reaction volume was fixed to 100 μl for all replicates and their controls. 1 μM ATP and 4 units of PKC-α (1 unit per 25 μl) were subsequently added. To initiate the phosphorylation reaction, 5 μl of PKC lipid activator (1:20 of reaction volume) containing 0.5 mg/ml phosphatidylserine and 0.05 mg/ml diacyglycerol in 20 mM MOPS (pH 7.2), 25 mM β-glycerol phosphate, 1 mM sodium orthovanadate, 1 mM dithiothretiol and 1 mM $CaCl_2$, was added. Two sets of control reactions were performed, one without PKC lipid activator and another with 0.1 μM PKC kinase inhibitor (GF 109203X), which were added before adding the kinase activator. PKC-α activity was measured by analysing the capacitance–voltage (*C–V*) characteristics of the $Si_3N_4/SiO_2/Si$ EIS structure. *C–V* measurements were performed using a CompactStat digital potentiostat (Ivium Technologies, The Netherlands). A conventional three-electrode electrochemical setup was employed with an Ag/AgCl reference electrode immersed in the electrolyte *via* a salt bridge used to apply the gate voltage and a Pt counter electrode. During the measurements, the gate voltage (V_g, applied between the reference electrode and the Al back-contact) was varied between -2 and +4 V, superimposed with a small ac signal of 10 mV at 1 kHz. The first measurement for the reaction was taken after adding ATP and kinase, i.e. before the start of phosphorylation process. After adding the kinase activator, the activity of the reaction was studied by recording the *C–V* characteristics every 2 minutes for 10 minutes. Finally, the measurements were taken at 20, 40 and 60 minutes after the start of the phosphorylation reaction. In the control reactions, *C–V* measurements were taken at similar time intervals. Each experiment was repeated at least three times and the reported data correspond to the average values. The maximum

observed value of the capacitance, C_{max}, which corresponds to $C_{dielectric}$ (capacitance of the silicon nitride / silicon dioxide dielectric layers) does not vary more than 3% from curve to curve. Therefore the curves have been normalized to C_{max} for ease of comparison.

Protein phosphorylation analysis using micro pH meters

For the direct pH measurements using the micro pH meter, the phosphorylation reactions and controls were carried out in solution using similar concentrations of the different components as before. The volume of the whole reaction was of 100 µl for all replicates and controls. An InLab Ultra Micro pH electrode with a S220 SevenCompact meter (Metter Toledo) was used to measure the pH of the reaction. This pH electrode has a tip of 3 mm diameter. The pH of the reaction was recorded every 2 minutes until 10 minutes and then at 20 minutes after the reaction. Each experiment was repeated three times and the average values are reported here.

Protein phosphorylation in solution and immunoblot-based detection

The phosphorylation reaction was done in suspension with the same concentrations as described for the phosphorylation on the silicon nitride surface in a 100 µl solution volume. Then 10 µl of reaction samples of phosphorylation and controls per lane were subjected to 12% acrylamide SDS-PAGE (polyacrylamide gel electrophoresis with sodium dodecyl sulphate). The proteins were electrophoretically transferred to a polyvinylidene fluoride (PVDF) membrane. Washing and hydration of the membrane was done using TBST buffer (10 mM Tris-HCl pH 7.5, 150 mM NaCl, Tween 20 0.001% V/v). The membranes were incubated at 4°C for 24 hours with phospho-(Ser) PKC substrate antibodies (1:1000) or 2 hours at room temperature with an anti-MBP antibody. A species-specific HRP-linked secondary antibody was then incubated for 45 minutes at room temperature. An enhanced chemiluminescence (ECL) method was used to detect the immunobands on the membranes.

TMB assay

MBP bio-functionalised Si_3N_4 surface was incubated with its antibody at a concentration of 0.5 $\mu g\,\mu l^{-1}$ for 30 minutes. The surface was then rinsed with 1 mM Tris buffer, pH 7.4, to remove excess of antibody. The unreacted sites of the protein were blocked with 5% bovine serum albumin (BSA) in

distilled H_2O. The sample was then incubated with 0.25 $\mu g\,\mu l^{-1}$ of secondary antibody linked with horseradish peroxidase (HRP) and then washed with 1 mM Tris buffer at pH 7.4. Two hundred microliter of TMB, T-4444 (3,3´,5,5´-tetramentylbenzidine) solution was dispensed on the Si_3N_4 surface and the samples were incubated at room temperature for 20 minutes until a distinct colour change was observed. Finally, the reaction was stopped by adding 50 µl of 2 M sulphuric acid and the absorbance was measurement at 450 nm using a low-volume spectrophotometer (Genova Nano, Jenway Biotech, USA).

Results and Discussion

Protein phosphorylation in solution and immunoblot-based detection

Using a conventional western blot technique we first confirmed the phosphorylation of MBP by the PKC-α kinase. This reaction was mainly done to optimize the reaction conditions, amount of kinase to be used and to identify the suitable buffer strength for the phosphorylation on the semiconductor structures. 2 gels were run with six lanes in each gel with phosphorylation reaction and controls. Lanes 2 through 6 had 10 µl of complete phosphorylation reaction with MBP, kinase and its activator. The difference between the lanes was in the buffer strength and its composition: reaction in lane 2 was done in 5 mM Tris base, pH 7.4, 150 mM NaCl and 10 mM $MgCl_2$; lane 3 reaction buffer was identical to lane 2 except it had 5% of BSA; lanes 4 and 5 differed from lanes 2 and 3 by using 1/5 of the amount of each buffer component (i.e. 1 mM Tris base, pH 7.4, 30 mM NaCl and 2 mM $MgCl_2$, with and without BSA). Lanes 1 and 6 had the control reactions: lane 1 was without kinase and lane 6 was without kinase activator. One gel was developed with phospho-tagged antibodies and another gel was developed with myelin basic protein antibodies. Fig 2A shows the data for phosphorylation of MBP. Luminescent bands were observed between 17 to 24 kDa, consistent with the MBP molecular weight of 18.2 kDa. No luminescence was observed in lanes 1 and 6 as shown in Fig 2A. After removing phospho-specific antibodies from the same blot, it was run with MBP antibodies to check whether MBP was present in lanes 1 and 6. Western blot on Fig. 2B shows that MBP was present in

all lanes. These results are consistent with the fact that phosphorylation of MBP was due to PKC-α kinase. It also depicts that PKC-α lipid activator is essential for activating kinase.

Phosphorylation on Si_3N_4

The immobilisation of MBP on the Si_3N_4 surfaces was demonstrated by adding an anti-MBP antibody followed by a HRP-modified secondary antibody. The TMB assay induces a colour change in the presence of HRP, which was detected using a spectrophotometer. The surface with immobilised MBP showed 10 times higher absorbance than the one without MBP (see supplementary information). Capacitance–voltage (*C–V*) characterisation of the EIS structures with MBP immobilised on the Si_3N_4 surface was also performed, revealing a pH sensitivity of 51.7 mV/pH between pH 7.2 and 8.8 (see supplementary information). For MBP in solution, there is a calculated change of net charge of +3.3 between pH 7.2 and 8.8, so a pH dependence of the *C-V* curves is expected since the change in charge affects the interfacial electrochemical potential, which in turn modulates the gate voltage. However, the main effect is likely to be associated with the known pH sensitivity of the Si_3N_4 dielectric: at lower pH values, the excess of H^+ ions on the Si_3N_4 surface decreases the threshold voltage of the structure; as a result, at higher pH the depletion region of the curve shifts towards lower gate voltages.

Fig 3A shows the changes in gate potential, ΔV_g, upon treatment of immobilised mylien basic protein with PKC-α kinase (4 units), its activator and ATP, at different time intervals. As the time interval for the interaction of MBP with PKC-α/ATP is extended, the changes in ΔV_g increase until it stabilises after 13 minutes to a value of 37 mV. Experiments without PKC-α kinase activator revealed a negligible change of 2.1 mV in gate potential (as seen in Fig. 3A). This implies that the kinase activator is essential to induce the chemical reaction on the bio-functionalised Si_3N_4 surface. The reaction with inhibitor did not show any significant changes in the ΔV_g, which was equal to 1.9 mV after 60 minutes. Upon phosphorylation of MBP by the kinase, each amino acid that undergoes phosphorylation releases a proton, which is adsorbed on the surface of Si_3N_4. As a result, the threshold potential of the structure decreases and a change in voltage is observed. As the reaction with kinase/ATP is prolonged, phosphorylation increases, leading to higher ΔV_g changes. The change in threshold potential was inversely proportional to the amount of phosphorylation. In Fig 3A the

saturation of surface groups observed after 13 minutes due to maximum kinase activity of 4 units leads to a stable value of ΔV_g equal to 37 mV.

The successful detection of the protein phosphorylation event was then tested to assay the kinase activity. The Si_3N_4 surface immobilised with MBP was reacted with different concentrations of PKC-α kinase in the presence of ATP and kinase activator for 40 minutes with a time interval of 2 minutes until 10 minutes and then at 20, 30 and 40 minutes after the start of the reaction. Fig 3B shows the change in gate voltage ΔV_g after maximum kinase activity was observed with different kinase concentrations. The shape of the curve depicts that a minimum of 0.5 units of kinase is required to see any noticeable potential change. However, 0.8-1 units of kinase are needed to yield a signal that distinguishes it from the controls (reactions with kinase inhibitor or without kinase activator) and confirm phosphorylation of protein.

Micro-pH electrode measurements

Fig 4 shows a pH change of 0.07 upon phosphorylation of MBP in solution, measured using a micro pH electrode. The pH of the solution containing kinase, ATP and MBP was found to be stable for at least 10 minutes. Upon the addition of the kinase activator, an abrupt change in pH was observed, which stabilised after 2 minutes for the next 20 minutes. This change was not observed without kinase activator or with inhibitor of kinase. Therefore we claim that changes in pH were due to phosphorylation of protein and can be detected using a micro-pH electrode. Overall the total change in pH detected was very low, at around 1.5%. This is attributed to the fact that the reaction is carried out in a buffer solution. The release of protons due to the phosphorylation reaction therefore disturbs only slightly the pH of the buffer. The pH value of 7.4 for the reaction solution was dictated by the need to retain the protein conformation and enable kinase activity. This indeed prevents high sensitivity responses. In addition, it was also apparent from the curves (Fig 4) that there was a long term drift and hysteresis losses in the sensor that resulted in slight pH changes when phosphorylation reaction is prolonged to check the stability. This accounts for the shape of the curve. However, 2-way ANOVA test revealed that phosphorylation results were significant when compared with the controls (without kinase activator and with kinase inhibitor) within $p < 0.01$. So this methodology still proves

to be a time and cost efficient in-laboratory technique that is able to distinguish between phosphorylated and non-phosphorylated substrates upon phosphorylation by kinase.

Detection mechanism on Si_3N_4

When hydrogen ions are released upon phosphorylation of protein, there is a change in pH of the solution which negates the negative charge on the protein due to phosphorylation. This is because when the pH decreases the net negative charge of the protein also decreases. This change in pH is measured by the Si_3N_4 EIS capacitor structure. The detection mechanism is similar to the operation of a field-effect transistor (FET). The difference lies in the removal of the metal layer from the gate of the FET, exposing the dielectric layers to direct contact with the electrolyte, whereby ions are adsorbed on the surface. This creates a conducting layer on the surface of the insulator and generates a similar effect to applying a voltage at the gate of a FET (F. Yan *et al.*, 2005). In particular, this can be explained by site binding theory, which relates the solid-liquid interface potential to local pH changes in the solution (Van Hal *et al.*, 1995; Wu *et al.*, 2013). At the interface, the Si_3N_4 surface has active sites in the form of neutral surface hydroxyl (SiOH) groups. Upon phosphorylation of MBP there is a release of a proton from every amino acid that gets phosphorylated. This release of H^+ ions is captured by SiOH groups until thermodynamic equilibrium is established between SiOH and H^+ ions released in the bulk electrolyte solution, as shown by the reaction

$$SiOH_2^+ \leftrightarrow SiOH + H^+$$

Equation 1 (Surmalyan, 2013) shows the dependence of the semiconductor surface potential (ϕ_s) on the hydrogen ion concentration:

$$\phi_s = -\frac{C_1}{C_h}(E_1 d_2 + E_2 d_2) + \phi_d + \frac{qN_{sil}}{C_h}\left\{\frac{[H_s^+]^2 - K_+K_-}{[H_s^+]^2 + K_+[H_s^+] + K_+K_-}\right\} + \frac{qN_{sil}}{C_h}\left\{\frac{[H_s^+]^2 - K_+K_-}{[H_s^+] + K_{N+}}\right\} \quad (1)$$

where C_1 is the accumulation capacitance due to the two dielectric layers, Si_3N_4 and SiO_2. $E_{1,2}$ and $d_{1,2}$ denote the electric field and thickness of each dielectric layer, respectively. C_h is the Helmholtz layer capacitance per unit area, N_{sil} is the number of silanol sites per unit area and $K_{+/-}$ are the dissociation constants for the chemical reaction at the insulator. It is apparent from the equation that highly

sensitive pH sensors would require relatively large N_{sil} values. The presence of two dielectric layers increases the pH sensitivity of the surface (Surmalyan, 2009). With two dielectric layers, as compared with a single insulator structure, the same concentration of H^+ ions on the surface yields higher surface potentials. Hence the increase in surface potential decreases the threshold seen by the channel at the transistor gate. As a result, at a given voltage the depletion charge increases at higher concentrations of H^+ ions.

Conclusions

This work successfully demonstrates and compares protein phosphorylation detection by pH-sensitive oxide-semiconductor capacitor structures and by a commercial micro-pH electrode. In particular, detection on pH-sensitive silicon nitride shows a remarkably high sensitivity and response. A good correlation was observed between our hypothesis and the experimental results. The generalized detection mechanism serves well to explain the detection of release of proton during protein phosphorylation. Direct detection of pH variations is challenging due to the buffering capabilities of the solution and to the technological difficulties in developing micro-pH electrodes which are subjected to less hydration and ion migration, and can measure local pH changes inside a buffer.

Although we studied phosphorylation of myelin basic protein by PKC-α, this approach can be extended for analysing activity of other kinases. The major potential application of this study would be the development of arrays of EIS structures, ISFETs or micro-pH sensors, whereby protein kinase activity is analysed in the presence of a wide range of inhibitors. This application would allow a giant leap forward in kinase inhibitor drug discovery. These label-free detection techniques might also prove useful to study protein kinase specificity (i.e. identification of target proteins amongst a subset of cellular proteins immobilised on a microchip), which would be of particular interest in cell biology and signalling research.

References

Arsenault, R., Griebel, P., Napper, S., 2011. Proteomics 11, 4595–4609.

Buxbaum, J.D., 1993. Proceedings of the National Academy of Sciences of the United States of America 90, 9195–9198.

Chen, R.-Q., Yang, Q.-K., Lu, B.-W., Yi, W., Cantin, G., Chen, Y.-L., Fearns, C., Yates, J.R., Lee, J.-D., 2009. Cancer Research 69, 2663–2668.

Chen, Z., He, X., Wang, Y., Wang, K., Du, Y., Yan, G., 2013. Biosensors and Bioelectronics 41, 519–525.

Cohen, P, 2001. European Journal of Biochemistry 268, 5001–5010.

Cohen, P., 2002. Nature Cell Biology 4, E127–130.

Cohen, P., Alessi, D.R., 2013. ACS Chemical Biology 8, 464–464.

Freeman, R., Gill, R., Willner, I., 2007. Chemical Communications,3450–3452.

Groban, E.S., Narayanan, A., Jacobson, M.P., 2006. PLoS Computational Biology 2, e32.

Van Hal, R.E.G., Eijkel, J.C.T., Bergveld, P., 1995. Sensors and Actuators B: Chemical 24, 201–205.

Inoue, H., Miyaji, M., Kosugi, A., Nagafuku, M., Okazaki, T., Mimori, T., Amakawa, R., Fukuhara, S., Domae, N., Bloom, E.T., Umehara, H., 2002. European Journal of Immunology 32, 2188–2198.

Kerman, K., Kraatz, H.-B., 2009. Biosensors and Bioelectronics 24, 1484–1489.

Kobashigawa, Y., Tomitaka, A., Kumeta, H., Noda, N.N., Yamaguchi, M., Inagaki, F., 2011. Proceedings of the National Academy of Sciences of the United States of America 108, 20579–20584.

Lindsay, S., 2012. Journal of Physics: Condensed Matter 24, 164201.

Manning, G., Whyte, D.B., Martinez, R., Hunter, T., Sudarsanam, S., 2002. Science 298, 1912–1934.

Mark, D., Haeberle, S., Roth, G., Von Stetten, F., Zengerle, R., 2010. Chemical Society Reviews 39, 1153–1182.

Martić, S., Beheshti, S., Kraatz, H.-B., Litchfield, D.W., 2012a. Chemistry and Biodiversity 9, 1693–1702.

Martić, S., Gabriel, M., Turowec, J.P., Litchfield, D.W., Kraatz, H.-B., 2012b. Journal of the American Chemical Society 134, 17036–17045.

Martinez, A., Castro, A., Dorronsoro, I., Alonso, M., 2002. Medicinal Research Reviews 22, 373–384.

Miao, P., Ning, L., Li, X., Li, P., Li, G., 2012. Bioconjugate Chemistry 23, 141–145.

Nadler, T.K., Rauh-Adelmann, C., Murphy, C., Hall, A.B., Graham, J.R., Yen, L., Gordon, N.F., Radding, J.A., 2008. Journal of Biomolecular Screening 13, 626–637.

Piehler, J., Brecht, A., Valiokas, R., Liedberg, B., Gauglitz, G., 2000. Biosensors and Bioelectronics 15, 473–481.

Rothberg, J.M., Hinz, W., Rearick, T.M., Schultz, J., Mileski, W., Davey, M., Leamon, J.H., Johnson, K., Milgrew, M.J., Edwards, M., Hoon, J., Simons, J.F., Marran, D., Myers, J.W., Davidson, J.F., Branting, A., Nobile, J.R., Puc, B.P., Light, D., Clark, T.A., Huber, M., Branciforte, J.T., Stoner, I.B., Cawley, S.E., Lyons, M., Fu, Y., Homer, N., Sedova, M., Miao, X., Reed, B., Sabina, J., Feierstein, E., Schorn, M., Alanjary, M., Dimalanta, E., Dressman, D., Kasinskas, R., Sokolsky, T., Fidanza, J.A., Namsaraev, E., McKernan, K.J., Williams, A., Roth, G.T., Bustillo, J., 2011. Nature 475, 348–352.

Stasyk, T., Huber, L.A., 2012. Trends in Molecular Medicine 18, 43–51.

Surmalyan, A.V., 2009. Armenian Journal of Physics 2, 326–332.

Surmalyan, A.V., 2013. Armenian Journal of Physics 5, 194–202.

Wang, D., Fu, Q., Zhou, Y., Xu, B., Shi, Q., Igwe, B., Matt, L., Hell, J.W., Wisely, E. V, Oddo, S., Xiang, Y.K., 2013. Journal of Biological Chemistry 288, 10298–10307.

Wang, J., Shen, M., Cao, Y., Li, G., 2010. Biosensors and Bioelectronics 26, 638–642.

Wang, J., Cao, Y., Li, Y., Liang, Z., Li, G., 2011. Journal of Electroanalytical Chemistry 656, 274–278.

Wieckowska, A., Li, D., Gill, R., Willner, I., 2008. Chemical Communications, 2376–2378.

Wu, M.-H., Yang, H.-W., Hua, M.-Y., Peng, Y.-B., Pan, T.-M., 2013. Biosensors and Bioelectronics 47, 99–105.

Yan, F., Estrela, P., Mo, Y., Migliorato, P., Maeda, H., Inoue, S., Shimoda, T., 2005. Applied Physics Letters 86, 053901.

Yoshida, T., Sato, M., Ozawa, T., Umezawa, Y., 2000. Analytical Chemistry 72, 6–11.

Zhang, D., Ortiz, C., Xie, Y., Davisson, V.J., Ben-Amotz, D., 2005. Spectrochimica Acta A 61, 471–475.

Figure captions

Fig. 1 - Scheme for analysis of protein phosphorylation: A) Field-effect device well for protein phosphorylation measurement; B1) Electrolytic insulator semiconductor (EIS) structure immobilised with protein; B2) Phosphorylated protein (negatively charged) and release of proton; C1) Capacitance vs. Gate Voltage characteristic curve of EIS; C2) Change in Gate Voltage corresponding to change in pH.

Fig. 2 - Western blot: A) phosphorylation reaction blot; B) protein check blot; lanes 1-6 differ only in the buffer composition and strength, 1: complete buffer without kinase, 2: complete buffer with complete reaction, 3: complete buffer + BSA with complete reaction, 4: low ionic strength buffer with complete reaction, 5: low ionic strength buffer + BSA with complete reaction, 6: complete buffer without kinase activator : complete buffer was composed of 150 mM NaCl, 5 mM Tris pH 7.4 and 10 mM $MgCl_2$. low ionic strength buffer was composed of 30 mM NaCl, 1 mM Tris pH 7.4 and 2 mM $MgCl_2$

Fig. 3 - Protein phosphorylation on Si_3N_4: A) Time-dependent changes in gate potential upon (a) phosphorylation of MBP by PKC-α, (b) control reaction without kinase activator and (c) in the presence of kinase inhibitor; The points represent the average values of replicates; the line is a guide to the eye. B) Kinase activity plot: phosphorylation with different kinase concentrations.

Fig. 4 - Protein phosphorylation measurement with a micro-pH electrode; 2-way ANOVA test where phosphorylation results are significant compared with the results of achieved without kinase activator and with kinase inhibitor within $p < 0.01$.

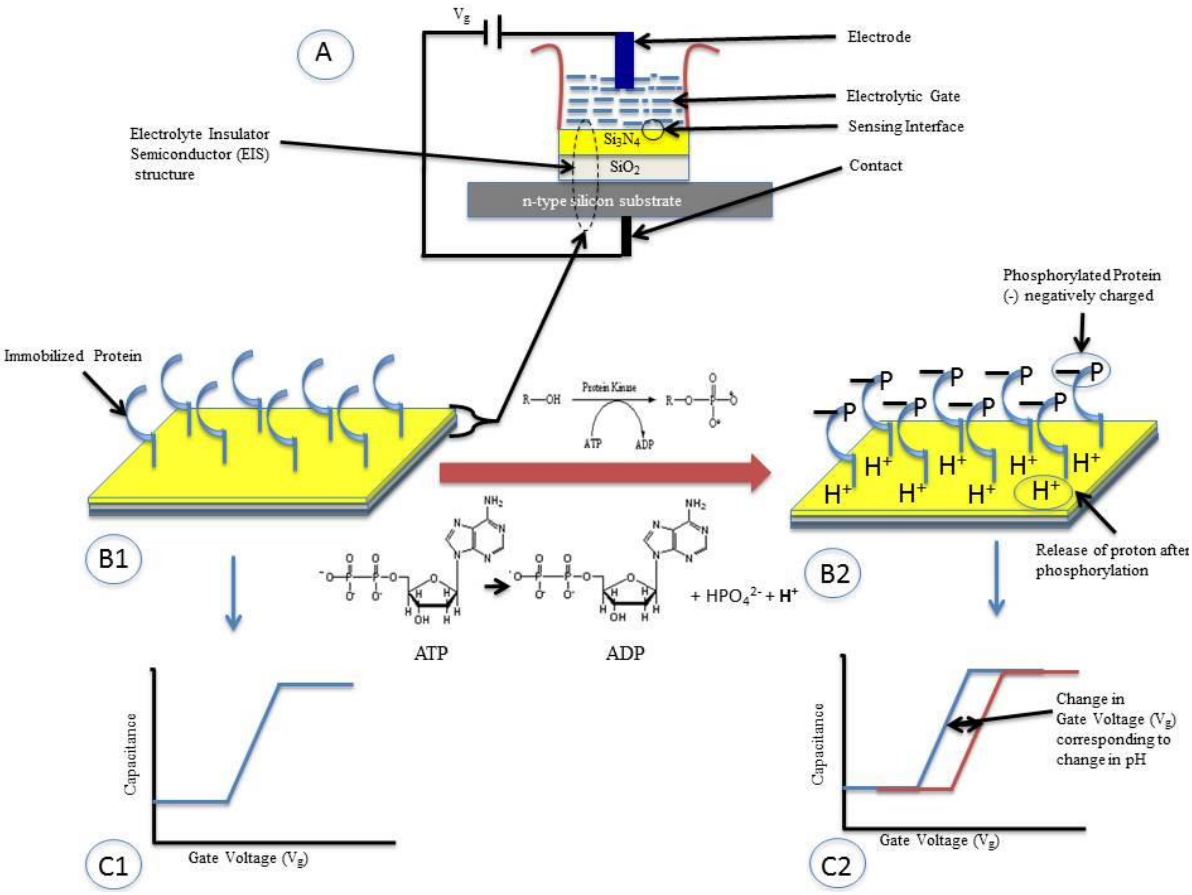

Figure 1

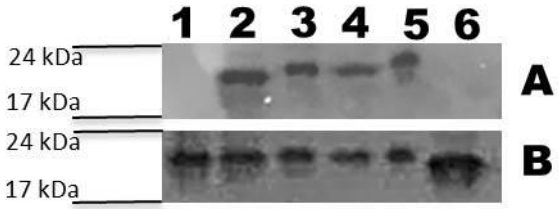

Figure 2

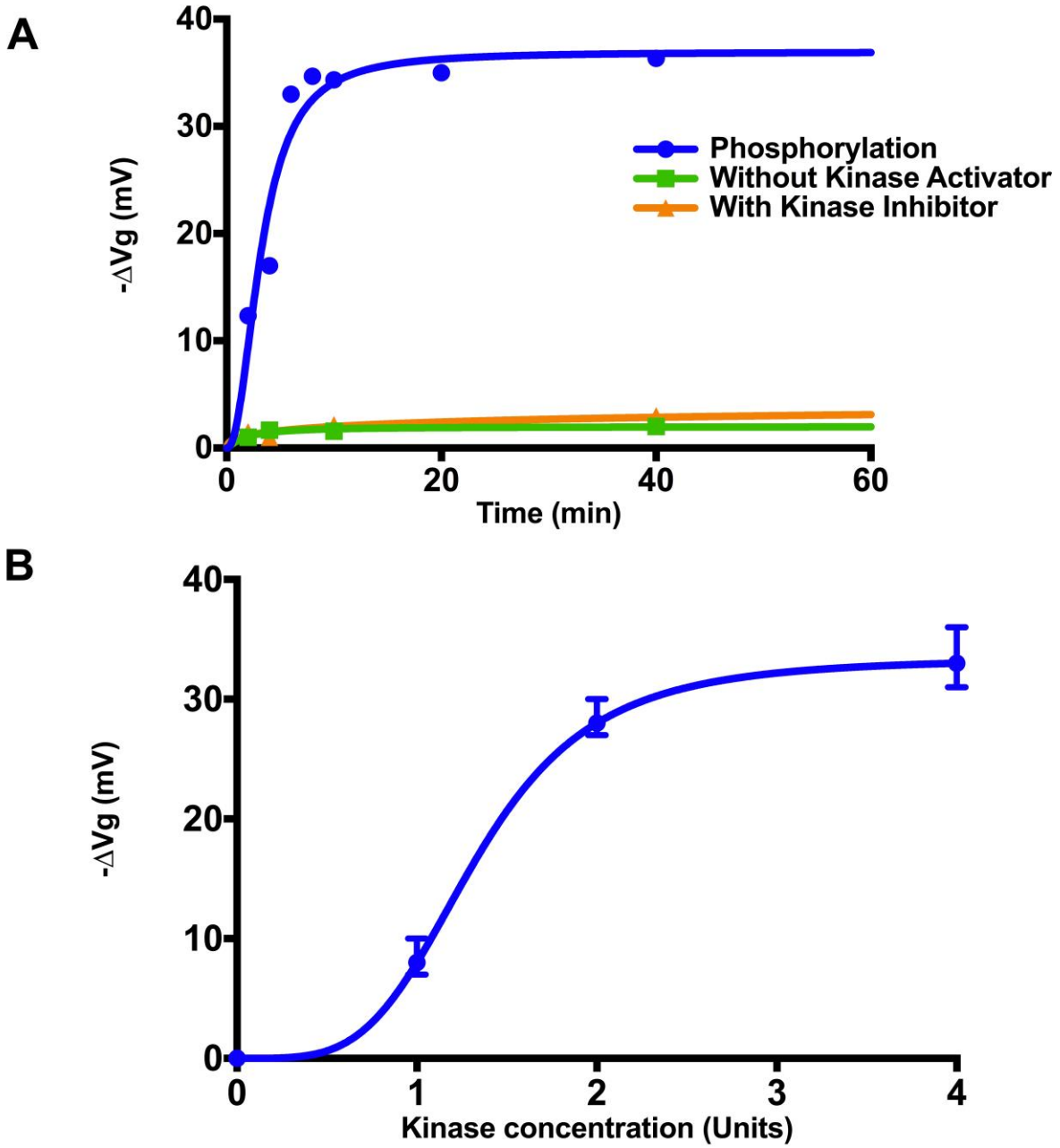
A
40
30
20
10
0
-ΔVg (mV)
0
20
40
60
Time (min)
Phosphorylation
Without Kinase Activator
With Kinase Inhibitor
B
40
30
20
10
0
-ΔVg (mV)
0
1
2
3
4
Kinase concentration (Units)

Figure 3

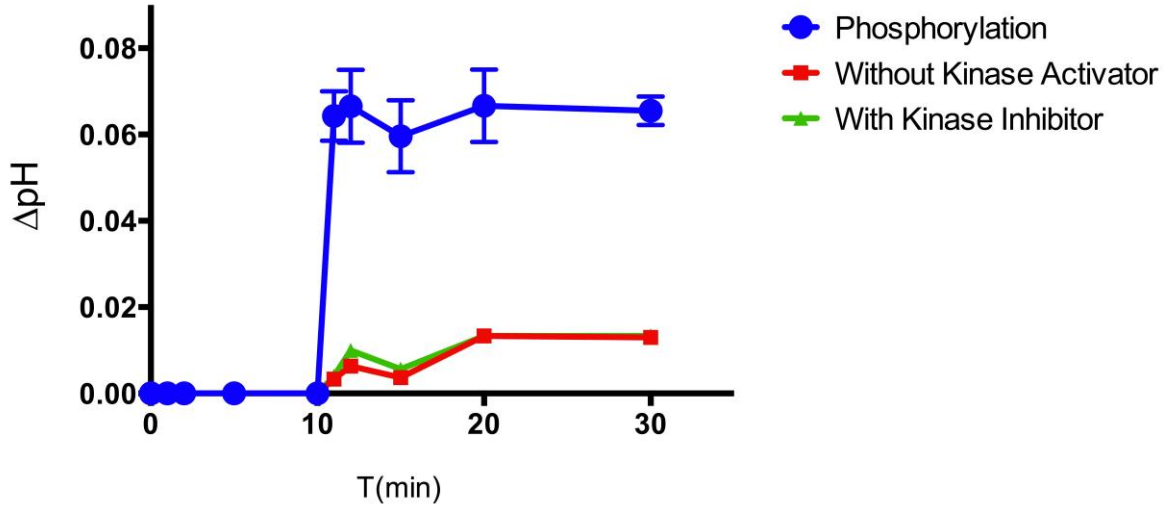
Phosphorylation
Without Kinase Activator
With Kinase Inhibitor
ΔpH
0.08
0.06
0.04
0.02
0.00
0
10
20
30
T(min)

Figure 4

Protein phosphorylation analysis based on proton release detection: potential tools for drug discovery

Nikhil Bhalla[1], Mirella Di Lorenzo[2], Giordano Pula[3], Pedro Estrela[1,*]

[1]Department of Electronic & Electrical Engineering, University of Bath, Bath BA2 7AY, United Kingdom

[2]Department of Chemical Engineering, University of Bath, Bath BA2 7AY, United Kingdom

[3]Department of Pharmacy & Pharmacology, University of Bath, Bath BA2 7AY, United Kingdom

Supplementary Information

The immobilisation of MBP on the Si_3N_4 surfaces was demonstrated by adding an anti-MBP antibody followed by a HRP-modified secondary antibody. The TMB assay induces a colour change in the presence of HRP, which was detected using a spectrophotometer. Fig. S1 shows a typical absorbance plot for the TMB assay where a peak was observed at 450 nm. The surface with immobilised MBP showed 10 times higher absorbance than the one without MBP.

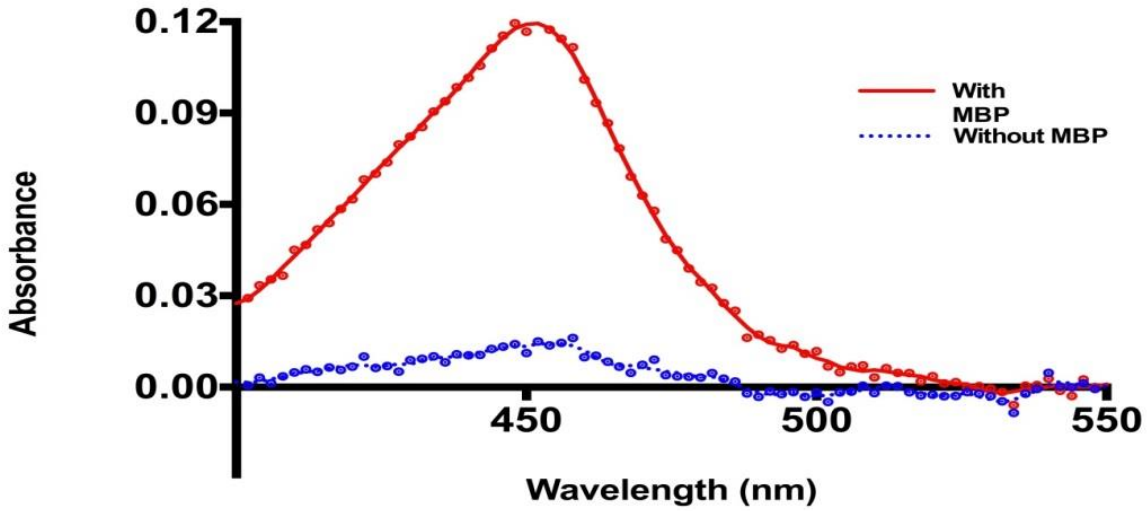

Fig. S1 - Immobilisation of myelin basic protein (MBP). The curve shows the absorbance peak at 450 nm for the TMB assay. The surface with immobilised MBP showed 10 times higher absorbance than the one without MBP. The lines are guides to the eye.

Capacitance–voltage (*C–V*) characterisation of the EIS structures with MBP immobilised on the Si_3N_4 surface was also performed, revealing a pH sensitivity of 51.7 mV/pH (Fig S2), using 1 mM Tris buffer at pH 8.8, 7.8 and 7.2. For MBP in solution, there is a calculated change of net charge of +3.3 between pH 7.2 and 8.8, so a pH dependence of the *C-V* curves

is expected since the change in charge affects the interfacial electrochemical potential, which in turn modulates the gate voltage. However, the main effect is likely to be associated with the known pH sensitivity of the Si_3N_4 dielectric. In Fig. S2, for a given voltage in the depletion region, an increase in capacitance is observed at higher pH. This is attributed to the fact that at lower pH, the excess of H^+ ions on the Si_3N_4 surface decreases the threshold voltage of the structure. As a result, at higher pH the depletion region of the curve shifts to the left as shown in Fig. S2. This shift indicates a change in the gate voltage, ΔV_g, which increases as pH decreases. This increase with pH was found to be linear with a regression coefficient of 0.99. The data in Fig. S2 served as calibration curves corresponding to the change in gate potential due to the change in pH.

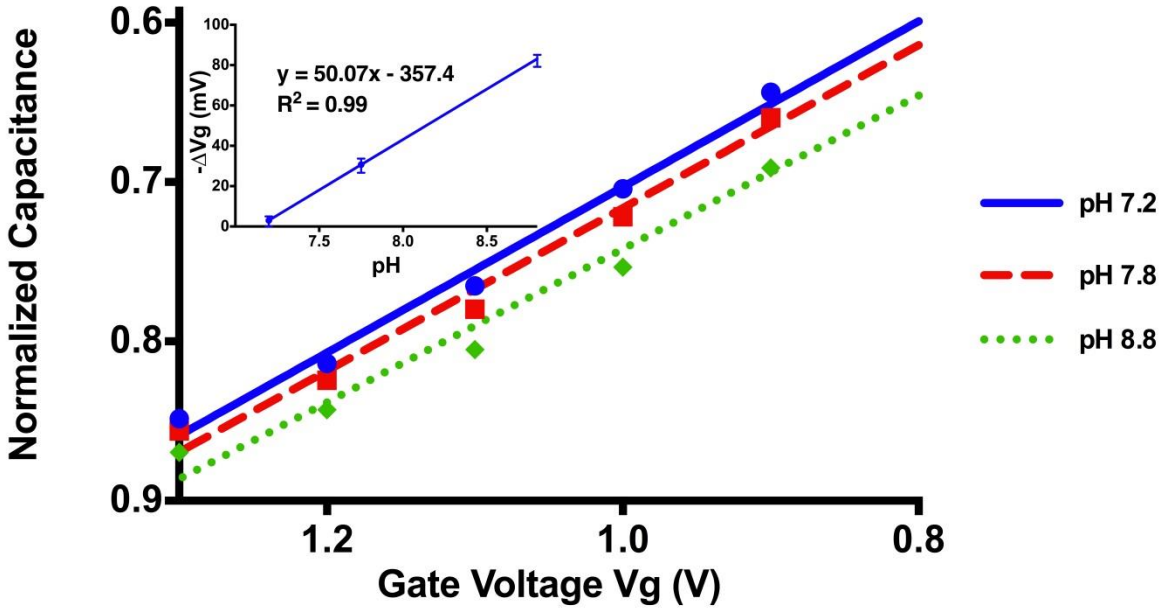

Fig.S 2 - Capacitance–voltage (*C–V*) characterisation of the EIS structures with MBP immobilised on the Si_3N_4 surface was also performed, revealing a pH sensitivity of 51.7 mV/pH, using 1 mM Tris buffer at pH 8.8, 7.8 and 7.2. The curves have been normalized for statistical comparison since $C_{dielectric}$ (capacitance of silicon nitride and silicon dioxide) does not vary more than 3% from curve to curve.

Experimental Setup

Fig S3 shows the experimental setup used. Reactions on silicon nitride were done by sandwiching the substrate between an upper Teflon well and a lower conducting plate. A conventional electrochemical setup with three electrodes was used to perform the Capacitance–voltage characterisation.

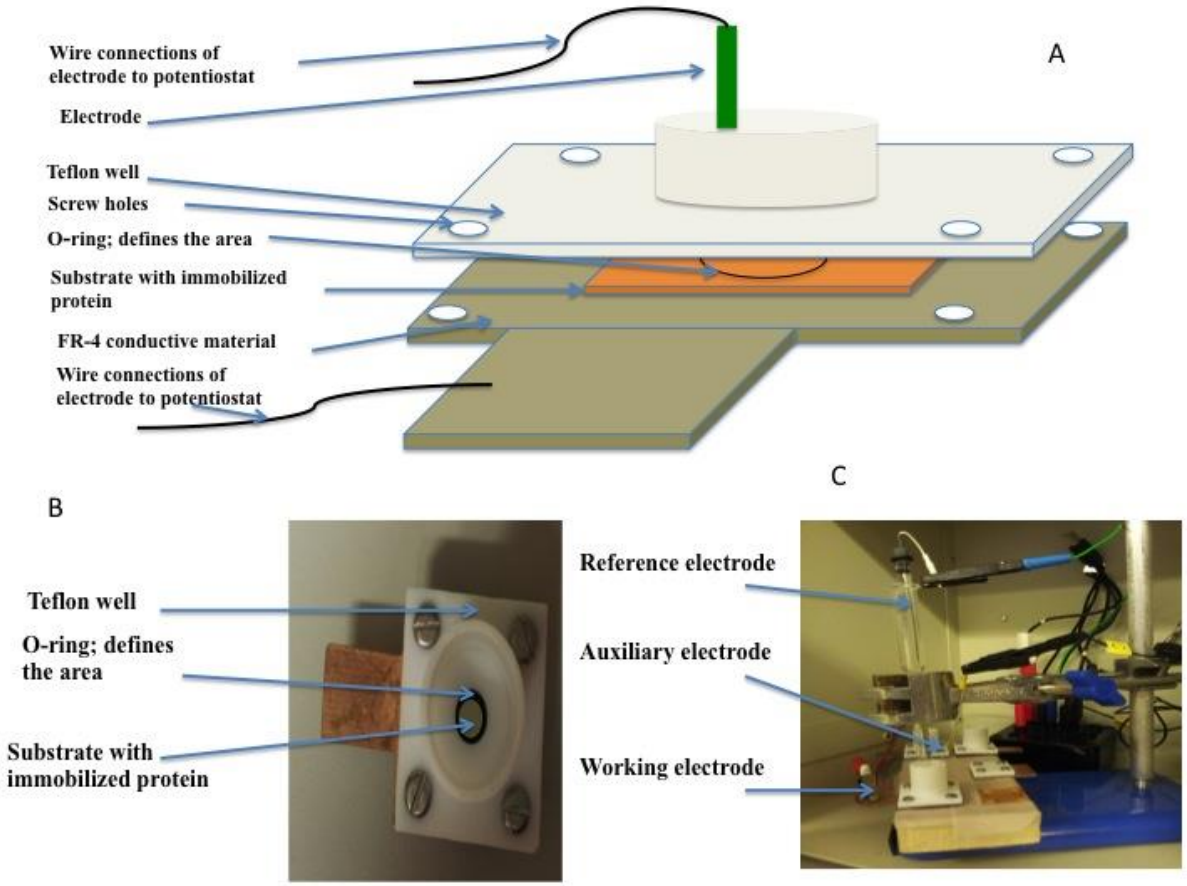

Fig S3 . Experimental Setup: (A) Detailed schematic of the reaction platform; (B) reaction platform; (C) three electrode system inside a Faraday cage.